ARTICLE

Quasi-classical Trajectory Study of C+CD→C$_2$+D at Different Collision Energy

Ying Shi[a*], Ting-xian Xie[b], Ming-xing Jin[a]

a. *Institute of Atomic and Molecular Physics, Jilin University, Changchun 130012, China*
b. *Dalian Jiaotong University School of Science, Dalian 116028, China*

Quasi-classical trajectory calculations have been employed to investigate the influence of collision energy on the stereodynamics of the title reaction C+CD→C$_2$+D on the potential energy surface of the $1^2A'$ state developed by Boggio-Pasqua *et al.* [Mol. Phys. **98**, 1925 (2000)]. The product angular distributions which reflect the vector correlation have been calculated. In addition, two polarization-dependent different cross-sections are also presented in the center-of-mass frame respectively. The results indicate that the product C$_2$ is sensitively affected by collision energy.

Key words: Quasi-classical trajectory, Stereodynamics calculation, Polarization dependent generalized differential cross-section, Stereodynamics

I. INTRODUCTION

Atom molecule reactions are important in a number of interesting situations including interstellar chemistry and upper atmosphere reactions [1, 2]. As a typical atom molecule reaction, the reaction C+CH→C$_2$H→C$_2$+H is selected mainly based on its importance in atmospheric chemistry and combustion [3−5]. Futhermore, the reaction can be considered as the prototype system to test the quality of new theories and experiments. Thus, the study of the reaction dynamics has received much attention recently, both experimentally [6−12] and theoretically [13−18].

Experimentally, in 1964, C$_2$H was first detected in argon matrixes [8]. Later, there have been extensive spectroscopic studies which mutually promoted the development of the understanding of the spectroscopy of C$_2$H [10, 11]. Using LIF method, Sorkhabi *et al.* studied the photodissociation of C$_2$H and estimated the branching ratios between the channels [12]. Theoretically, Boggio-Pasqua *et al.* presented the accurate adiabatic PESs by CASSCF calculations [13]. And the three lowest PESs are denoted $1^2A'$, $2^2A'$, and $1^2A''$ [13, 14]. In order to understand the dynamics of the reaction C+CH fully, it is important to gain not only its scalar properties, but also its vector properties. In 2001, the time-dependent quantum wave packet method has been used to study the reaction C+CH on the 1A′ and 2A′ surface by Tang *et al.* [15, 16]. Recently, the stereodynamics of the C+CH, the vector correlations and

polarization-dependent different cross-sections (PDD-CSs) dependence on the collision energy and different PESs have been carried out by the quasi-classical trajectory (QCT) method [17, 18].

In order to obtain more information of this reaction, we investigated the C+CD→C$_2$+D system by the QCT method. We performed the theoretical dynamics calculations of the title reaction on the $1^2A'$ PES, and analyzed the influence of the collision energies on the stereodynamics of this reaction.

II. THEORY

A. Quasi-classical trajectory calculations and potential energy surface

The calculated method in this work is the same as those described in the Refs. [19−22]. The QCT calculations code used in this work was provided by Professor Ke-li Han. The classical Hamilton's equations were integrated numerically for motion in three dimensions. In our calculation, the collision energy ranging from 0.1 eV to 0.3 eV, with sixth order symplectic integration by running batches of 2×10^4 trajectories. The trajectories were initialed at an C−CD internucleus separation of 10 Å. Vibrational and rotational levels of the reactants molecule are taken as $v=0$ and $j=0$, respectively. And the integration step size of 0.1 fs is used. In order to verify the accuracy of the numerical integration, the conservation of the total energy and total angular momentum for each trajectory has been checked.

In the present work, the product rotational polarization for the title reaction has been studied on the $1^2A'$ PES constructed by Boggio-Pasqua *et al.* [14]. The

---

*Author to whom correspondence should be addressed. E-mail: shi_ying@jlu.edu.cn, Tel.: +86-431-85168817
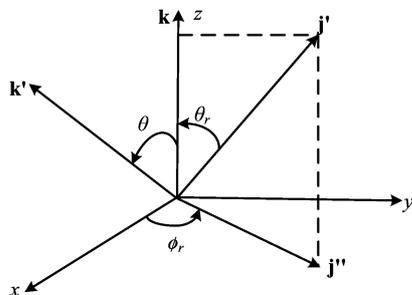
FIG. 1 The centre-of-mass coordinate system used to describe the **k**, **k'**, and **j'** distributions of the title reation.

advantage of this PES is that the saddle-point energy is lowered to 22.45 kJ/mol and removed the spurious features of the initial one [13].

B. Product rotational polarization

The full angular distribution of the triple vector correlations **k**, **k'**, **j'** of the product molecule are represented in the Fig.1 in the center-of-mass coordinate. In this coordinate, the reagent relative velocity **k** is parallel to the z-axis, and the y-axis is perpendicular to the x-z plane which contains the **k** and product relative velocity vector **k'**. In order to fully describe the vector correlation of the reaction, the correlated center-of-mass function was written as [23−25].

$$P\left(\cos\theta, \cos\theta_r, \phi_r\right) = \frac{1}{4\pi} \sum_{k=0}^{\infty} \sum_{q=-k}^{k} (2k+1) \cdot$$
$$\frac{2\pi}{\sigma} \frac{d\sigma_{kq}}{d\omega_t} C_{kq}\left(\theta_r, \phi_r\right)^* \qquad (1)$$

In Eq.(1), $\omega_t = \theta_t$, ϕ_t and $\omega_r = \theta_r$, ϕ_r which are the polar coordinates of the unit vectors k' and j' in the CM frame. σ is the integral cross section and $C_{kq}(\theta_r, \phi_r)$ represents the modified spherical harmonics. $(1/\sigma)(d\sigma_{kq}/d\omega_t)$ is used to decribed the generalized PDDCSs. The detail functional form in this work can be refered to the literature [26−28]. In our investigation, we are only interested in the two PDDCSs $(2\pi/\sigma)(d\sigma_{00}/d\omega_t)$ and $(2\pi/\sigma)(d\sigma_{20}/d\omega_t)$. The PDDCSs are expanded to $k=7$ for good convergence.

The usual two vector **k**-**j'** correlation distribution function $P(\theta_r)$ which can be used to expand in a series of Legendre polynomials [29−31].

$$P(\theta_r) = \frac{1}{2} \sum_k [k] a_0^k P_k\left(\cos\theta_r\right) \qquad (2)$$

To understand the three vector correlation, the dihedral angle distributions of the **k-k'-j'**, **k-k'-l**, and **k-k'-l'** are characterized by the angle ϕ_r, **l** (the reagent orbital angular momentum), and **l'** (the product orbital angular momentum), respectively. The distribution function
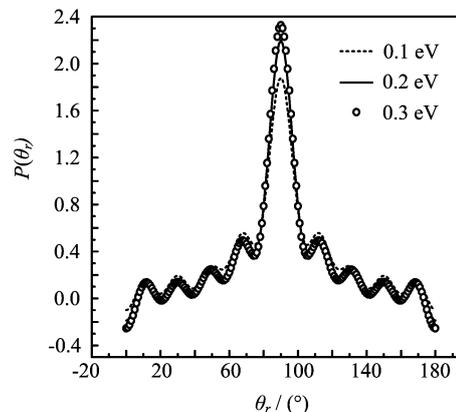

FIG. 2 The distributions of $P(\theta_r)$ reflecting **k-j'** correlation at three collision energies.

$P(\phi_r)$ can be expanded as a Fourier series [32−34].

$$P(\phi_r) = \frac{1}{2\pi}\left(1 + \sum_{n_{\text{even}} \geq 2} a_n \cos n\phi_r + \right.$$
$$\left. \sum_{n_{\text{odd}} \geq 1} b_n \sin n\phi_r \right) \qquad (3)$$

The joint probability density function $P(\theta_r, \phi_r)$ reflecting the spatial distributions of product rotational angular momenta is given as follows:

$$P\left(\theta_r, \phi_r\right) = \frac{1}{4\pi} \sum_{kq} [k]\, a_q^k C_{kq}\left(\theta_r, \phi_r\right)^*$$
$$= \frac{1}{4\pi} \sum_k \sum_{q \geq 0} \left(a_{a\pm}^k \cos q\phi_r - a_{q\mp}^k i \sin q\phi_r\right) \cdot$$
$$C_{kq}\left(\theta_r, 0\right) \qquad (4)$$
$$a_n = 2\langle \cos n\phi_r \rangle \qquad (5)$$
$$b_n = 2\langle \sin n\phi_r \rangle \qquad (6)$$

III. RESULTS AND DISCUSSION

The calculated results of distribution of $P(\theta_r)$ dependence on collision energies of the title reaction are shown in Fig.2. The global reaction is barrierless relative to the reagent channel. We selected the collision energies at E_T=0.1, 0.2, and 0.3 eV. As we can see from Fig.2, the peak of $P(\theta_r)$ is at θ_r=90° and symmetric about the right angle which can be attributed to the planar symmetry of the system. The observed results suggest that the product rotational angular momentum vector of the title reaction is strongly aligned along the direction perpendicular to the relative velocity direction. There is a contraction of the $P(\theta_r)$ with the peak moving upwards, thus indicating the product rotational alignment effect becomes stronger with increasing of collision energies.
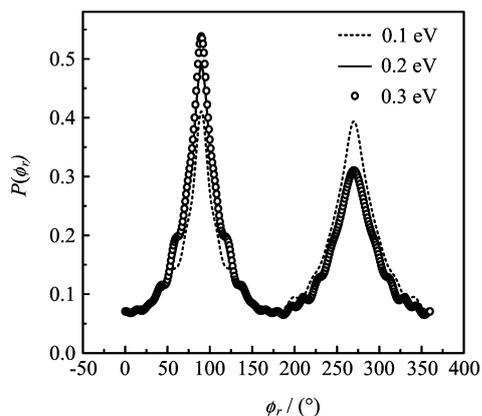
FIG. 3 The distribution of $P(\phi_r)$ discribes the dihedral angle distribution of $\mathbf{j}'$ with respect to the $\mathbf{k}$-$\mathbf{k}'$ plane at three collision energies.

The difference of $P(\theta_r)$ distributions dependence on the collision energies is in accordance with the results of the product rotational alignment parameter $\langle P_2(j',k)\rangle$. The calculated values of $\langle P_2(j',k)\rangle$ was -0.473, -0.482, and -0.485 with increasing collision energies ranging from 0.1 eV to 0.3 eV respectively, which leads to the stronger product rotational alignment.

In Fig.3, the dihedral angle distribution presenting the correlation of the $\mathbf{k}$-$\mathbf{k}'$-$\mathbf{j}'$ has been calculated. There are two peaks at 90° and 270°. The peak at 90° becomes higher with increasing collision energies, while the opposite tendency occure at 270°. At the 0.1 eV collision energy, the two peaks values almost the same. With the increasing of collision energies, considering the difference of the two peak at 90° and 270°, we can deduce that the product rotational angular momentum vector $\mathbf{j}'$ not only aligned, but also oriented along the y-axis. It is clear that the $P(\phi_r)$ distribution is asymmetric, which is probably attributed to the effect of the repulsive energy between C−D atoms. According to the previous theoretical "impulsive collision model" [35−37], the distribution of the product rotational angular momentum vector j',

$$j' = L\sin^2\beta + j\cos^2\beta + J_1 m_A/m_B \qquad (7)$$

$$J_1 = (\mu_{BC}R)^{1/2} r_{AB} r_{CB} \qquad (8)$$

where L is the reagent orbital angular momentum, μ_{BC} is the reduced mass of the BC molecular and R is the repulsive energy. In the title reaction, the term of $L\sin^2\beta + j\cos^2\beta$ is symmetric while the $J_1 m_A/m_B$ term show a preferring direction for the effect of repulsive energy, which leads to the left handed product rotation in planes parallel to the scattering plane. The peak of 90° increases with increasing of the collision energy, which can also be explained by the repulsive model. As described above, J_1 plays a crucial role in the product rotational orientation, large J_1 thus leads to stronger orientation along the J_1 direction. Because
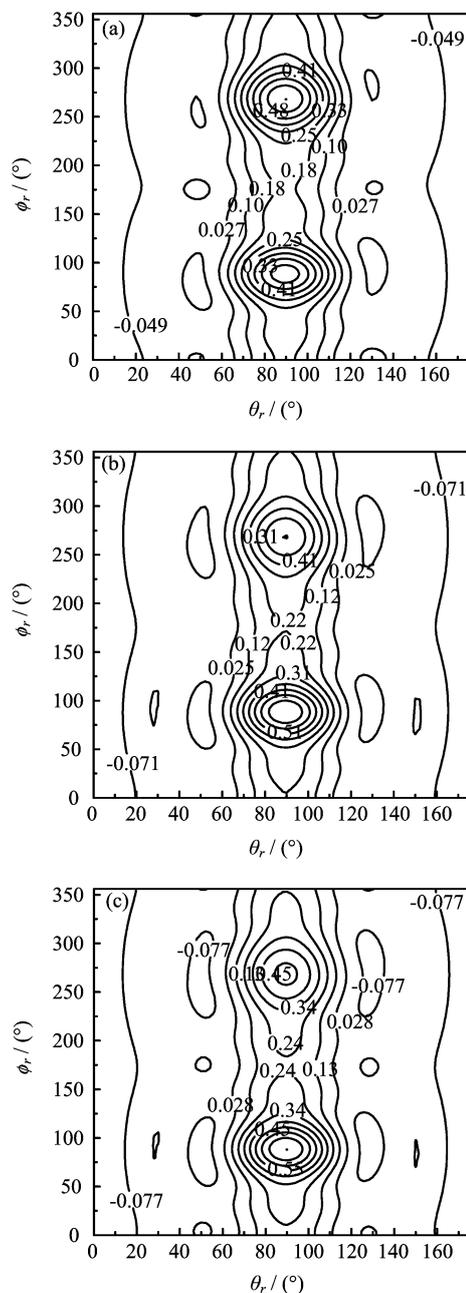

FIG. 4 Polar plots of $P(\theta_r,\phi_r)$ distribution averaged over all scattering angles for three collision energies. (a) E_T=0.1 eV, (b) E_T=0.2 eV, (c) E_T=0.3 eV.

the repulsive energy R increases with the collision energy, we can see that the modulus of J_1 becomes larger at high collision energy. Therefore, this influence plays a dominant part in product rotational orientation at high collision energy, thereby leading to the orientation along the positive direction of y-axis [38, 39].

The topographical features of the $P(\theta_r,\phi_r)$ distributions can be used to further support the above-mentioned vector correlations about the influence of collision energies differences on the stereodynamics of the
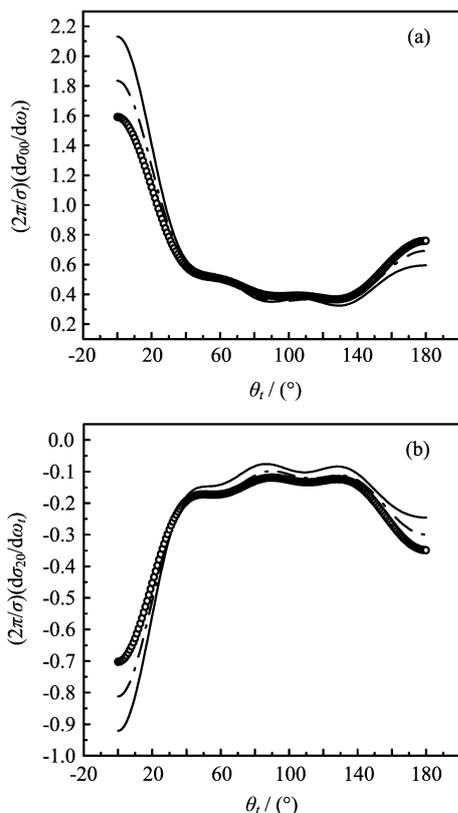
FIG. 5 The two PDDCSs of the title reation. Solid, dash, and circle lines correspond to the reaction of collision energies 0.1, 0.2, and 0.3 eV, respectively.

zero, which indicates that the rotational angular momentum distribution is more isotropic than these scattering angles. This behavior is almost invariant for three collision energies. The conclusion of product angular momentum $\mathbf{j}'$ strongly aligned perpendicular to $\mathbf{k}$ at 0° and 180° for the three collision energies also can be deduced.

IV. CONCLUSION

In this work, the stereodynamics of the reaction C+CD→C_2+D has been investigated by the QCT method. We present the vector correlation of $P(\theta_r)$, $P(\phi_r)$, and $P(\theta_r, \phi_r)$. There is a contraction of the $P(\theta_r)$ with the peak moving upwards, thus indicating the product rotational alignment effect becomes stronger with increasing of collision energies. With the increasing of collision energies, considering the difference of the two peak of $P(\phi_r)$ at 90° and 270°, we can deduce that the product rotational angular momentum vector $\mathbf{j}'$ not only aligned, but also oriented along the y-axis. In addition, with the increasing of collision energies, degree of PDDCSs forward scattering whereas that of backward scattering is also strongly affected by collision energies.

V. ACKNOWLEDGMENTS

title reaction. As can be seen from Fig.4, the distributions of $P(\theta_r, \phi_r)$ with a peak at $(90°, 270°)$ are in good accordance with the distributions of $P(\theta_r)$ and $P(\phi_r)$ of the C_2 products for three collision energies.

Figure 5 plottes the generalized PDDCSs which are used to depict the $\mathbf{k}$-$\mathbf{k}'$-$\mathbf{j}'$ correlation and the scattering direction of the products as a function of scattering angle θ_t. The PDDCSs of product $(2\pi/\sigma)(\mathrm{d}\sigma_{00}/\mathrm{d}\sigma_{\omega_t})$ and $(2\pi/\sigma)(\mathrm{d}\sigma_{20}/\mathrm{d}\sigma_{\omega_t})$ are drawn in Fig.5. Further, PDDCSs are not completely symmetric with a forward scattering bias. The backward-forward asymmetry may be attributed to the exothermic feature of the reactions. As simple the differential cross-section, the PDDCS $(2\pi/\sigma)(\mathrm{d}\sigma_{00}/\mathrm{d}\sigma_{\omega_t})$ shown in Fig.5(a) only describes the $\mathbf{k}$-$\mathbf{k}'$ correlation or the scattering direction of the product, and is not associated with the orientation and alignment of the product rotational angular momentum vector $\mathbf{j}'$. Figure 5(a) present that the product is almost exclusively forward and backward scattering for three collision energies. With the increasing of collision energies, degree of forward scattering decreases slightly whereas that of backward scattering increases slightly. Figure 5(b) shows the behavior of $(2\pi/\sigma)(\mathrm{d}\sigma_{20}/\mathrm{d}\sigma_{\omega_t})$ which give the opposite trend to that of $(2\pi/\sigma)(\mathrm{d}\sigma_{00}/\mathrm{d}\sigma_{\omega_t})$. Far away from the scattering angles 0° and 180°, we observed that the value of the PDDCS become close to

[1] I. Glassman, *Combustion*, 3rd ed., New York: Academic, 56 (1996)
[2] D. G. Truhlar, J. T. Muckerman, *Atom-Molecules Collision Theory*, R. B. Bernstein, Ed., New York: Plenum Press, 505 (1979).
[3] Y. C. Hsu, J. M. Lin Jr., D. Papoušek, and J. J. Sai, J. Chem. Phys. **98**, 6690 (1993).
[4] D. L. Lambert, Y. Sheffer, A. C. Danks, C. Arpigny, and P. Magain, Astrophys. J. **353**, 476 (1990).
[5] W. M. Jackson, Y. Bao, and R. S. Urdahl, J. Geophys. Res. **96**, 17569 (1991).
[6] Y. C. Hsu, Y. J. Shin, and C. M. Lin, J. Chem. Phys. **103**, 5919 (1995).
[7] W. B. Yan, H. E. Warner, and T. Amano, J. Chem. Phys. **94**, 1712 (1991).
[8] E. L. Cochran, F. J. Adrian, and V. A. Bowers, J. Chem. Phys. **40**, 213 (1964).
[9] T. A. Cool and P. M. Goodwin, J. Chem. Phys. **94**, 6978 (1991).
[10] M. E. Jacox, Chem. Phys. **7**, 424 (1975).
[11] J. M. Brown and K. M. Evenson, J. Mol. Spectrosc. **131**, 161 (1988).

[12] O. Sorkhabi, V. M. Blunt, H. Lin, D. Xu, J. Wrobel, R. Price, and W. M. Jackson, J. Chem. Phys. **107**, 9842 (1997).

[13] M. Boggio-Pasqua, A. I. Voronin, P. Halvick, J. C. Rayez, and A. J. C. Varandas, Mol. Phys. **98**, 1925 (2000).

[14] M. Boggio-Pasqua, P. Halvick, M. T. Rayez, J. C. Rayez, and J. M. Robbe, J. Phys. Chem. A **102**, 2009 (1998).

[15] B. Y. Tang, M. D. Chen, K. L. Han, and J. Z. H. Zhang, J. Chem. Phys. **115**, 731 (2001).

[16] B. Y. Tang, M. D. Chen, K. L. Han, and J. Z. H. Zhang, J. Phys. Chem. A **105**, 8629 (2001).

[17] H. H. Zhang, C. J. Hu, Q. Wei, and B. Zhang, Mol. Phys. **107**, 2503 (2009).

[18] H. R. Zhang, Z. Y. Liu, S. H. Sun, L. Li, H. C. Du, and B. T. Hu, J. Theor. Comput. Chem. **10**, 75 (2011).

[19] K. L. Han, L. Zhang, D. L. Xu, G. Z. He, and N. Q. Lou, J. Phys. Chem. A **105**, 2956 (2001).

[20] M. L. Wang, K. L. Han, and G. Z. He, J. Phys. Chem. A **103**, 10204 (1999).

[21] M. D. Chen, K. L. Han, and N. Q. Lou, J. Chem. Phys. **118**, 4463 (2003).

[22] M. D. Chen, K. L. Han, and N. Q. Lou, Chem. Phys. Lett. **357**, 483 (2002).

[23] T. S. Chu, Y. Zhang, and K. L. Han, Int. Rev. Phys. Chem. **25**, 201 (2006).

[24] K. L. Han, G. Z. He, and N. Q. Lou, J. Chem. Phys. **105**, 8699 (1996).

[25] J. Zhao, Y. Xu, and Q. T. Meng, J. Phys. B **42**, 165006 (2009).

[26] Y. F. Liu, Y. L. Gao, D. H. Shi, and J. F. Sun, Chem. Phys. **364**, 46 (2009).

[27] W. W. Xu, X. G. Liu, and Q. G. Zhang, Mol. Phys. **106**, 1787 (2008).

[28] S. L. Liu and Y. Shi, Chem. Phys. Lett. **501**, 197 (2011).

[29] W. L. Li, M. S. Wang, C. L. Yang, W. W. Liu, C. Sun, and T. Q. Ren, Chem. Phys. **337**, 93 (2007).

[30] Q. Wei, X. Li, and T. Li, Chem. Phys. **368**, 58 (2010).

[31] L. Yao, Y. L. Liu, H. Y. Zhong, and W. H. Cao, J. Theor. Comput. Chem. **8**, 827 (2009).

[32] H. Z. Sun, X. G. Liu, J. J. Lv, and H. R. Liu, Chin. J. Chem. Phys. **23**, 521 (2010).

[33] X. A. Jing, C. L. Yang, M. S. Wang, and X. G. Ma, Chem. Phys. **379**, 46 (2011).

[34] T. S. Chu, Y. Zhang, and K. L. Han, Int. Rev. Phys. Chem. **25**, 201 (2006).

[35] Y. Xu, J. Zhao, D. G. Yue, H. Liu, X. J. Zheng, and Q. T. Meng, Chin. Phys. B **18**, 5308 (2009).

[36] C. H. Zhang, W. Q. Zhang, and M. D. Chen, J. Theor. Comput. Chem. **8**, 403 (2009)

[37] X.F. Yue, J. Cheng, H. Feng, H. Li, and E. L. Wu, Chin. J. Chem. Phys. **23**, 381 (2010).

[38] W. Q. Zhang, S. L. Cong, C. H. Zhang, X. S. Xu, and M. D. Chen, J. Phys. Chem. A **113**, 4192 (2009).

[39] W. Q. Zhang, Y. Z. Li, X. S. Xu, and M. D. Chen, Chem. Phys. **367**, 115 (2010).